CONSTRUCTIVE MATHEMATICAL ANALYSIS
7 (2024), No. SI, pp. 50-00
http://dergipark.org.tr/en/pub/cma
ISSN 2651 - 2939

Research Article

Analytical results for a linear hardening elasto-plastic spring investigated via a hemivariational formulation

Dedicated to Professor Paolo Emilio Ricci, on occasion of his 80th birthday, with respect and friendship.

LUCA PLACIDI*, ANIL MISRA, ABDOU KANDALAFT, MOHAMMAD MAHDI NAYEBAN, AND NURETTIN YILMAZ

ABSTRACT. We investigate the linear hardening phenomena with a method that is not standard in the literature, i.e. with a hemivariational method. As a result, we do not introduce any flow rules, and the number of assumptions is reduced to the generalized variational principle with proper definition of a new set of kinematic descriptors and, as a function of them, with a new definition of the energy functional. The variational framework guarantees the rationality of the deduction. Analytical derivation of the force displacement hysteretic loop is also derived and, finally, the dissipation energy is furnished with respect to either the final value of the dissipation energy potential or the corresponding area of the hysteretic loop.

Keywords: Linear hardening, hysteretic loop, variational method, plasticity.

2020 Mathematics Subject Classification: code, code.

1. INTRODUCTION

Linear hardening behavior of a class of materials is well-known in the literature [7, 21], and the methods for its study are also explored in many aspects [74, 75]. However, we will examine the possibility of a new approach with some advantages. The first is that the number of assumptions is reduced, and the second is that analytical solutions [18, 78] are derived with no use of flow rules. We need to say that elastic models can be derived in different ways, i.e. by assuming the balance of forces, of moments and therefore of the corresponding Partial Differential Equations (PDEs) and Boundary Conditions (BCs) as first principles or by assuming an energetic approach, where the assumptions are based on an action principle, and the PDEs and BCs are derived as a consequence of these first assumptions [8, 27, 23, 36, 32]. In standard continuum elastic models, fundamental problems arise, see e.g. [19, 49, 50], as well as the necessity of higher order gradient generalization [4, 35, 1] also for the dynamic case [33, 57]. These kinds of generalizations are particularly important for materials with microstructures, made e.g. with additive manufacturing techniques [10, 11, 12], for fiber-reinforced composites [13, 29, 46, 52, 51, 69], for composite structure [34], and for biological applications [43, 44, 76, 61, 2]. Thus, variational approaches have been developed also for microstructural materials [26, 28]. Also thermomechanical problems [53, 56, 70, 72] can be used via a purely variational procedure [40]. Besides, the use of 3D printers has improved the investigation of metamaterials, made with a microstructure that can be designed, as pantographic

Received: 13.08.2024; Accepted: 15.10.2024; Published Online: 16.12.2024
*Corresponding author: Luca Placidi; luca.placidi@uninettunouniversity.net
DOI: 10.33205/cma.1532828

materials [15, 24, 25, 31, 80], where higher order gradient is essential for the modelling. Higher order gradient elastic theories are therefore suitable for those materials with microstructure. However, the number of constitutive parameters of a general higher order gradient theory is so large that the problem of their identification is an open one, and deserves specific techniques [38, 37]. In order to avoid the identification of a large number of parameters, one can use the same strategy of Cauchy and Navier [14, 62] for homogeneous linear and isotropic materials aimed to solve the elastic granular micromechanic problem [9] for anisotropic [30] and generalized continuous [45, 47, 64, 63, 81, 82]. Granular micromechanic is ideal for concrete [16, 17] and for any materials with a strengthening microstructure [20] with the necessity to model the bond behavior [48]. Variational principles for elastic materials are therefore standard. For the dissipative case, e.g. for the viscoelastic case [41, 42, 54], the variational strategy must be generalized [71, 5, 65]. For damage [83, 77, 79] and plasticity [3] such a strategy is also different. Variational approaches in plasticity are not new [39, 22, 55]. The aim of this work is to use a hemivariational procedure, conceived for granular micromechanics [59, 58, 60, 66, 67], for a one degree of freedom problem with linear hardening behavior. Such a one degree of freedom model can be used into two ways to construct a continuum model with the same linear hardening behavior. The first is to build a discrete mode and use standard homogenization technique [68, 73]. The second is to use granular micromechanics [66]. As an outlook of this work, we will consider the fatigue problem [6].

2. Formulation of the problem

2.1. **Definition of the Action functional and plastic kinematic descriptors.**

The action A

$$A = \int_{t_{in}}^{t_{fi}} \left\{ U + W - U^{ext} \right\} dt \tag{2.1}$$

is a functional of the fundamental kinematical quantities u, λ_t, and λ_c, i.e. of the functions, $\hat{u}$, $\hat{\lambda}_t$ and $\hat{\lambda}_c$,

$$A = \mathcal{A}\left(\hat{u}, \hat{\lambda}_t, \hat{\lambda}_c\right). \tag{2.2}$$

$\hat{u}$, $\hat{\lambda}_t$, and $\hat{\lambda}_c$ are all functions of time t (where t_{in} is the initial time and t_{fi} is the final time),

$$u = \hat{u}\left(t\right), \qquad \lambda_t = \hat{\lambda}_t\left(t\right), \qquad \lambda_c = \hat{\lambda}_c\left(t\right), \qquad \forall t \in \left[t_{in}, t_{fi}\right], \tag{2.3}$$

and called, respectively, the displacement and plastic multipliers in tension and compression. The plastic multipliers are also called, respectively, the tension and the compression plastic displacement accumulations. The reason for these names is as follows. The elastic displacement u_{el}

$$u_{el} = u - u_{pl}, \tag{2.4}$$

is defined as the difference between the total displacement u and the plastic displacement u_{pl}, that is defined as the difference between the tension and compression plastic accumulations, i.e. between the two plastic multipliers, viz.,

$$u_{pl} = \lambda_t - \lambda_c. \tag{2.5}$$

The values U, W, and U^{ext} are the elastic, the dissipation, and the external energies which are functionals of the fundamental kinematical fields,

$$U = \mathcal{U}\left(\hat{u}, \hat{\lambda}_t, \hat{\lambda}_c\right), \quad W = \mathcal{W}\left(\hat{\lambda}_t, \hat{\lambda}_c\right), \quad U^{ext} = \mathcal{U}^{ext}\left(\hat{u}\right).$$

The explicit form of the functionals $\mathcal{U}$, $\mathcal{W}$ and $\mathcal{U}^{ext}$ is prescribed constitutively. Here we restrict to the condition that the dissipation energy functionals depend only upon the plastic multipliers and the external energy functional $\mathcal{U}^{ext}$ only upon the total displacement.

2.2. **Kinematic and thermodynamic restrictions of motion.**

2.2.1. *Boundary conditions in time.* An initial datum on plastic multipliers must be assumed at $t = t_{in}$,

$$\lambda_{t0} = \hat{\lambda}_t\left(t = t_{in}\right), \quad \lambda_{c0} = \hat{\lambda}_c\left(t = t_{in}\right), \tag{2.6}$$

as well as initial and final displacements,

$$u_{in} = \hat{u}\left(t_{in}\right), \qquad u_{fi} = \hat{u}\left(t_{fi}\right), \tag{2.7}$$

both at the initial $t = t_{in}$ and at the final $t = t_{fi}$ instants of times. Conditions (2.7) can also be omitted in the present quasi-static formulation but they should be taken into account when the kinetic energy in (2.1) is considered.

2.2.2. *Definition of motion.* A motion is defined as a family, fulfilling (2.6) and (2.7), of displacements $u = \hat{u}\left(t\right)$ and of plastic multipliers $\lambda_t = \hat{\lambda}_t\left(t\right)$ and $\lambda_c = \hat{\lambda}_c\left(t\right)$ for those discrete values of times defined as follows,

$$t = t_i = t_{in} + i\Delta t, \qquad \forall i = 0, \ldots, N, \qquad t_{in} = t_0, \qquad t_{fi} = t_N = t_0 + N\Delta t.$$

The increments, across two successive instants of times, of displacement

$$\Delta u = \hat{u}\left(t_{i+1}\right) - \hat{u}\left(t_i\right), \tag{2.8}$$

and of plastic multipliers

$$\Delta\lambda_t = \hat{\lambda}_t\left(t_{i+1}\right) - \hat{\lambda}_t\left(t_i\right), \quad \Delta\lambda_c = \hat{\lambda}_c\left(t_{i+1}\right) - \hat{\lambda}_c\left(t_i\right), \tag{2.9}$$

at time $t = t_i$ are defined in (2.8) and (2.9).

2.2.3. *Admissible variation of motion.* The set AM_t is that of kinematically admissible displacements $(2.3)_1$, fulfilling the (2.7) in the non-quasi-static case and any kinematical restrictions imposed by the problem, e.g., by the external constraints, at time t. The set AV_t is that of their admissible variations,

$$u \in AM_t, \qquad \delta\hat{u} \in AV_t.$$

Two examples are as follows. The first is for a force-control problem, where the displacement u is not prescribed, the variation $\delta\hat{u}$ is arbitrary, and we have

$$AV_t \equiv \mathbb{R}, \qquad \forall t \in \left(t_{in}, t_{fi}\right)$$

for any values of time, in the non-quasi-static case different from the initial and the final ones because of (2.7). The second is for a displacement-control problem, where the displacement is prescribed, and the only admissible value for its variation $\delta\hat{u}$ is zero, i.e. $\delta\hat{u} = 0$; as a consequence the set of admissible variations

$$AV_t = \{0\}, \qquad \forall t \in \left[t_{in}, t_{fi}\right]$$

is composed only of the zero value. The kinematical quantities λ_t and λ_c are assumed to be irreversible and therefore can not reduce their values. Thus, their admissible variations are all the positive numbers, viz.,

$$\delta\hat{\lambda}_t \in \mathbb{R}^+, \quad \delta\hat{\lambda}_c \in \mathbb{R}^+. \tag{2.10}$$

The kinematical irreversibility of the plastic multipliers justifies the relation of their names with the accumulation of tension and compression plastic displacements. It is worth noting

that the plastic displacement defined in (2.5) is not irreversible. The irreversibility conditions on the two plastic multipliers that are assumed in (2.10), induce the necessity to generalize the variational principle into a hemivariational principle, that is discussed in the next subsection.

2.3. **The hemivariational principle.** The variation $\delta\mathcal{A}$ of the action functional (2.2) is defined with respect to the variations of the kinematic descriptors (2.3),

$$\delta\mathcal{A} = \mathcal{A}\left(\hat{u}+\delta\hat{u}, \hat{\lambda}_t+\delta\hat{\lambda}_t, \hat{\lambda}_c+\delta\hat{\lambda}_c\right) - \mathcal{A}\left(\hat{u}, \hat{\lambda}_t, \hat{\lambda}_c\right), \tag{2.11}$$

and its increment $\Delta\mathcal{A}$ is defined with respect to those increments defined in (2.8) and (2.9), that yields

$$\Delta\mathcal{A} = \mathcal{A}\left(\hat{u}+\Delta\hat{u}, \hat{\lambda}_t+\Delta\hat{\lambda}_t, \hat{\lambda}_c+\Delta\hat{\lambda}_c\right) - \mathcal{A}\left(\hat{u}, \hat{\lambda}_t, \hat{\lambda}_c\right). \tag{2.12}$$

The hemivariational principle is formulated as follows: The following variational inequality holds

$$\Delta\mathcal{A} \leq \delta\mathcal{A} \tag{2.13}$$

for the solution (2.3) and for any admissible variations

$$\forall\delta\hat{u} \in AV_t, \qquad \forall\delta\hat{\lambda}_t \in \mathbb{R}^+, \quad \forall\delta\hat{\lambda}_c \in \mathbb{R}^+. \tag{2.14}$$

Finally, the only thermodynamic restriction, among the positive definiteness of the elastic energy functional $\mathcal{U}$, involves the dissipation energy, that is assumed to be a non-decreasing function of time,

$$\Delta\mathcal{W}\left(\hat{\lambda}_t, \hat{\lambda}_c\right) = \mathcal{W}\left(\hat{\lambda}_t+\Delta\hat{\lambda}_t, \hat{\lambda}_c+\Delta\hat{\lambda}_c\right) - \mathcal{W}\left(\hat{\lambda}_t, \hat{\lambda}_c\right) \geqslant 0. \tag{2.15}$$

3. The case of an elasto-plastic linear kinematic hardening spring

3.1. **Definition of the energy functionals.** The elastic energy is assumed to be quadratic with respect to the elastic displacement u_{el} defined in (2.4) and proportional to the elastic stiffness k_{el}, i.e.,

$$U = \mathcal{U}\left(\hat{u}, \hat{\lambda}_t, \hat{\lambda}_c\right) = \frac{1}{2}k_{el}u_{el}^2 = \frac{1}{2}k_{el}\left(u-u_{pl}\right)^2 = \frac{1}{2}k_{el}\left(u-\lambda_t+\lambda_c\right)^2. \tag{3.16}$$

The dissipation energy is defined with the following incomplete quadratic form of the irreversible plastic kinematic descriptors,

$$W = \sigma\left(\lambda_t+\lambda_c\right) + \frac{1}{2}h\left(\lambda_t-\lambda_c\right)^2, \tag{3.17}$$

where σ is the initial plastic yielding point, and h is the hardening parameter. Positive definition of the numbers of the three constitutive coefficients of the model, i.e.,

$$k_{el} > 0, \qquad \sigma > 0, \qquad h > 0,$$

guarantees not only the positive definiteness of the elastic energy functional $\mathcal{U}$ but also the assumed thermodynamic restriction (2.15).

The external energy

$$U^{ext} = \mathcal{U}^{ext}\left(\hat{u}\right) = Fu, \tag{3.18}$$

is defined with the external force F, that is a function of time,

$$F = \hat{F}\left(t\right). \tag{3.19}$$

Thus, the action functional is given by the insertion of (3.16), (3.17) and (3.18) into (2.1)

$$\mathcal{A} = \int_{t_{in}}^{t_{fi}} \left[\frac{1}{2} k_{el} \left(u - \lambda_t + \lambda_c \right)^2 + \sigma \left(\lambda_t + \lambda_c \right) + \frac{1}{2} h \left(\lambda_t - \lambda_c \right)^2 - Fu \right] dt, \tag{3.20}$$

and its variation is,

$$\begin{aligned} \delta\mathcal{A} = \int_{t_{in}}^{t_{fi}} \{ & \left[k_{el} \left(u - \lambda_t + \lambda_c \right) - F \right] \delta\hat{u} \\ & + \left[-k_{el} \left(u - \lambda_t + \lambda_c \right) + \sigma + h \left(\lambda_t - \lambda_c \right) \right] \delta\hat{\lambda}_t + \left[k_{el} \left(u - \lambda_t + \lambda_c \right) + \sigma - h \left(\lambda_t - \lambda_c \right) \right] \delta\hat{\lambda}_c \} dt, \end{aligned}$$

or, in compact form,

$$\delta\mathcal{A} = \int_{t_{in}}^{t_{fi}} \{ \left[k_{el} \left(u - u_{pl} \right) - F \right] \delta\hat{u} + \left[k_{el} + h \right] \left[\left(\lambda_t - \lambda_{ty} \right) \delta\hat{\lambda}_t + \left(\lambda_c - \lambda_{cy} \right) \delta\hat{\lambda}_c \right] \} dt, \tag{3.21}$$

where λ_{ty} and λ_{cy} are the plastic yielding tension and the plastic yielding compression, respectively, i.e.,

$$\lambda_{ty} = \lambda_c + \frac{k_{el} u - \sigma}{k_{el} + h}, \tag{3.22}$$

$$\lambda_{cy} = \lambda_t - \frac{k_{el} u + \sigma}{k_{el} + h}. \tag{3.23}$$

The increment $\Delta\mathcal{A}$ of the action functional (2.12) is derived from (3.21),

$$\Delta\mathcal{A} = \int_{t_{in}}^{t_{fi}} \{ \left[k_{el} \left(u - \lambda_t + \lambda_c \right) - F \right] \Delta\hat{u} + \left[k_{el} + h \right] \left[\left(\lambda_t - \lambda_{ty} \right) \Delta\hat{\lambda}_t + \left(\lambda_c - \lambda_{cy} \right) \Delta\hat{\lambda}_c \right] \} dt. \tag{3.24}$$

3.2. **Euler-Lagrange equations for the linear kinematic hardening spring.** The variational inequality (2.13) is valid for any admissible variations in (2.14). Let us define an arbitrary function of time $f \in AV_t$ belonging to the admissible displacement variations AV_t and calculate the variational inequality (2.13) with the following admissible variation

$$\left(\delta\hat{u}, \delta\hat{\lambda}_t, \delta\hat{\lambda}_c \right) = \left(f, \Delta\hat{\lambda}_t, \Delta\hat{\lambda}_c \right),$$

and then with another admissible variation that is similar to the previous one but with opposite f, i.e.,

$$\left(\delta\hat{u}, \delta\hat{\lambda}_t, \delta\hat{\lambda}_c \right) = \left(-f, \Delta\hat{\lambda}_t, \Delta\hat{\lambda}_c \right),$$

both for arbitrary $f \in AV_t$. Thus, we obtain two inequalities, that imply the following Euler-Lagrange equation

$$\left[k_{el} \left(u - \lambda_t + \lambda_c \right) - F \right] f = 0, \qquad \forall f \in AV_t, \tag{3.25}$$

that, by assuming no restrictions on $f \in AV_t$, we easily derive the standard form of the elasto-plastic linear kinematic hardening spring response,

$$k_{el} \left(u - \lambda_t + \lambda_c \right) = k_{el} \left(u - u_{pl} \right) = F. \tag{3.26}$$

Thus, let us calculate the variational inequality (2.13) by assuming the following particular admissible variation evaluated on the corresponding increment of the solution but doubling that of the tension plastic multiplier,

$$\left(\delta\hat{u}, \delta\hat{\lambda}_t, \delta\hat{\lambda}_c\right) = \left(\Delta\hat{u}, 2\Delta\hat{\lambda}_t, \Delta\hat{\lambda}_c\right), \tag{3.27}$$

and then with another admissible variation that is similar to the previous one but keeping the plastic multiplier in tension at zero,

$$\left(\delta\hat{u}, \delta\hat{\lambda}_t, \delta\hat{\lambda}_c\right) = \left(\Delta\hat{u}, 0, \Delta\hat{\lambda}_c\right). \tag{3.28}$$

It is easy to derive that the two obtained inequalities imply another Euler-Lagrange equation for the plastic multiplier in tension in the form of the following KKT condition,

$$\left[\lambda_t - \lambda_{ty}\right] \Delta\lambda_t = 0. \tag{3.29}$$

In the same way we obtain the other plastic KKT conditions,

$$\left[\lambda_c - \lambda_{cy}\right] \Delta\lambda_c = 0. \tag{3.30}$$

It is worth to be noted that the variations (3.27) and (3.28) are both admissible because the increments on the solutions are always non-negative as it is prescribed in (2.14). Besides, a variation $\delta\hat{\lambda}_t = -\Delta\hat{\lambda}_t$, for the same reason, is not admissible.

3.3. **A resume of the governing equations.** The governing equations of the present linear hardening spring are given by the coupling effects of eqns. (3.26), (3.29) and (3.30) with the insertion, respectively, of (2.5), (3.22) and (3.23),

$$\left[\lambda_t - \lambda_c - \frac{k_{el}u - \sigma}{k_{el} + h}\right] \Delta\lambda_t = 0, \tag{3.31}$$

$$\left[\lambda_c - \lambda_t + \frac{k_{el}u + \sigma}{k_{el} + h}\right] \Delta\lambda_c = 0, \tag{3.32}$$

$$k_{el}\left(u - \lambda_t + \lambda_c\right) = F. \tag{3.33}$$

The explicit method consists of the following numerical strategy once the displacement history u is prescribed for all the time steps. From (3.31), we evaluate λ_t by assuming the other multiplier λ_c at the previous time step. Thus, from (3.32), we evaluate λ_c by assuming the other multiplier λ_t at the previous time step. Finally, we calculate the reaction F from (3.33) and repeat this scheme for every time steps.

4. The cycling loading of the elasto-plastic linear kinematic hardening spring

4.1. **The cyclic loading history.** The cyclic loading history is prescribed in terms of the displacement field and graphically represented in Fig. 1. The period of oscillation of the imposed displacement is $4\bar{t}$. The oscillation range is $2\overline{u}$, where $\overline{u}$ is assumed to be larger than σ/k_{el}.

We investigate, in the following six subsections of Section 4, the six phases of the loading history. We will call these stages of the loading history as follows: elastic reversible one, plastic irreversible one, elastic reversible two, plastic irreversible two, elastic reversible three, and plastic irreversible three. We will later justify the names of these phases. It is worth noting here that in the elastic phases, the dissipation energy is constant with respect to time, and in the plastic phases, the dissipation energy is an increasing function with respect to time. Besides, on the one hand, during the elastic phases, an eventual unloading process follows the loading path (reversibility of the process), and on the other hand, during the plastic phases, an eventual unloading process follows another path (irreversibility of the process).

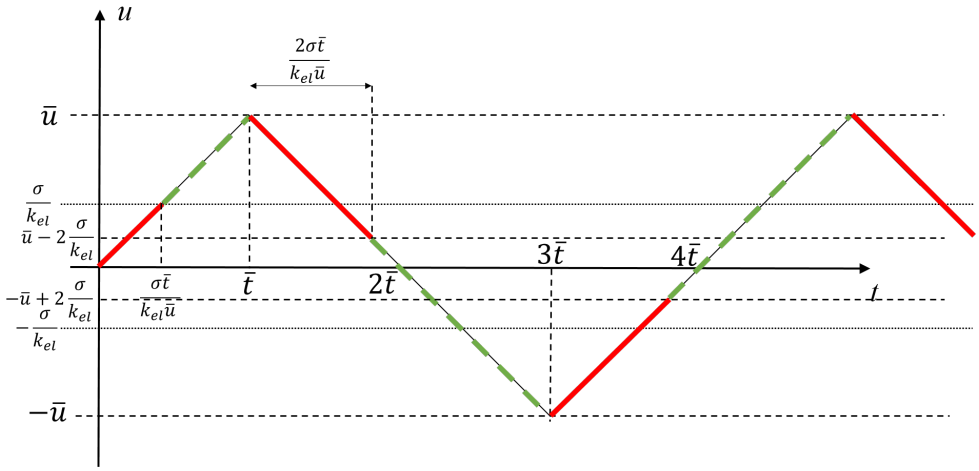

FIGURE 1. The cyclic loading history in terms of the imposed displacement u vs the time t. Each period is divided into six phases. Three phases (red-thick lines) are denoted elastic and three (green-dashed lines) are denoted plastic.

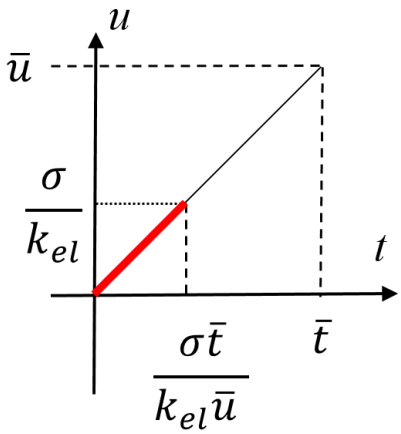

FIGURE 2. Elastic reversible phase one of the loading history in terms of the imposed displacement u vs time t.

4.2. **Elastic reversible phase one.** At the beginning of the loading history (i.e. at $t = t_{in} = 0$) the displacement and both the plastic multipliers are null

$$u\left(t = t_{in} = 0\right) = \lambda_c\left(t = t_{in} = 0\right) = \lambda_t\left(t = t_{in} = 0\right) = 0. \tag{4.34}$$

Besides, the displacement u is imposed to evolve according to Fig. 1, and it is therefore limited, in the elastic reversible phase one, to be

$$u < \frac{\sigma}{k_{el}}, \qquad \forall t \in [0, \frac{\sigma\bar{t}}{k_{el}\bar{u}}], \tag{4.35}$$

lower than the ratio σ/k_{el} as remarked in Fig. 2. Besides, the plastic yielding tension and

compression are at the beginning from (3.22), (3.23) and (4.34) both negative,

$$\lambda_{ty}\left(t=t_{in}=0\right)=-\frac{\sigma}{k_{el}+h}<0,\qquad \lambda_{cy}\left(t=t_{in}=0\right)=-\frac{\sigma}{k_{el}+h}<0. \tag{4.36}$$

On the one hand, from (3.23) and because u is an increasing function of time for this elastic reversible phase one (see Fig. 2), the plastic yielding compression λ_{cy} is a decreasing function of time, which guarantees that it is constrained to be negative for all the times in this initial part of the loading history,

$$\dot{u}>0,\quad \Rightarrow\quad \dot{\lambda}_{cy}=-\frac{k_{el}\dot{u}}{k_{el}+h}<0,\quad \Rightarrow\quad \lambda_{cy}\left(t\right)<0,\qquad \forall t\in[0,\frac{\sigma\bar{t}}{k_{el}\bar{u}}].$$

Thus, the KKT condition (3.30) is satisfied only by setting to zero the increment $\Delta\lambda_c$ and therefore also the values of the plastic multiplier in compression λ_c for all the times in this initial part of the loading history,

$$\lambda_c\left(t\right)=0,\qquad \forall t\in[0,\frac{\sigma\bar{t}}{k_{el}\bar{u}}]. \tag{4.37}$$

On the other hand, from (3.22) and because u is an increasing function of time for this elastic reversible phase one (see Fig. 2), the plastic yielding tension λ_{ty} is an increasing function of time. However, from (3.22), (4.35) and (4.37), it remains negative for all times in this initial part of the loading history,

$$\lambda_{ty}\left(t\right)=\lambda_c+\frac{k_{el}u-\sigma}{k_{el}+h}=\frac{k_{el}u-\sigma}{k_{el}+h}<0,\qquad \forall t\in[0,\frac{\sigma\bar{t}}{k_{el}\bar{u}}].$$

Thus, also the KKT condition (3.29) is satisfied only setting to zero the increment $\Delta\lambda_t$ and therefore also the values of the plastic multiplier in tension for all the times in this initial part of the loading history,

$$\lambda_t\left(t\right)=0,\qquad \forall t\in[0,\frac{\sigma\bar{t}}{k_{el}\bar{u}}]. \tag{4.38}$$

The conditions (4.37) and (4.38) justify to call elastic this first part of the loading history. The spring response has been derived from (3.26), (4.37) and (4.38), and takes the following simple form

$$k_{el}u=F,\qquad \forall t\in[0,\frac{\sigma\bar{t}}{k_{el}\bar{u}}], \tag{4.39}$$

that is also represented in Fig. 3.

If, in an arbitrary moment of this elastic reversible phase we change the sign of the loading velocity $\dot{u}$ then the KKT conditions (3.29) and (3.30) will be both satisfied with the same constant values of plastic multipliers (4.37) and (4.38) and therefore the response is the same calculated in (4.39) and graphically reported in Fig. 3. This reversible behavior justifies the name "reversible" of this phase of the loading history.

4.3. **The plastic irreversible phase one.** In the second part of the loading history, the displacement u is imposed to evolve according to Fig. 1, and it is therefore limited, in the plastic irreversible phase one, to be

$$\frac{\sigma}{k_{el}}<u<\bar{u},\qquad \forall t\in[\frac{\sigma\bar{t}}{k_{el}\bar{u}},\bar{t}]$$

as represented in Fig. 4. Thus, the yielding compression from (3.23) is still a decreasing function

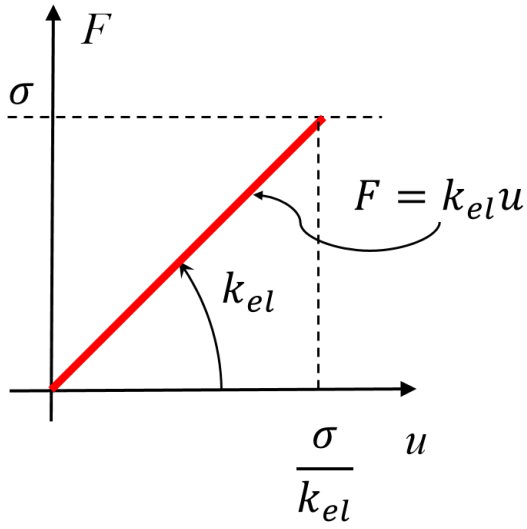

FIGURE 3. Elastic reversible phase one response. We plot the reaction force F vs the imposed displacement u.

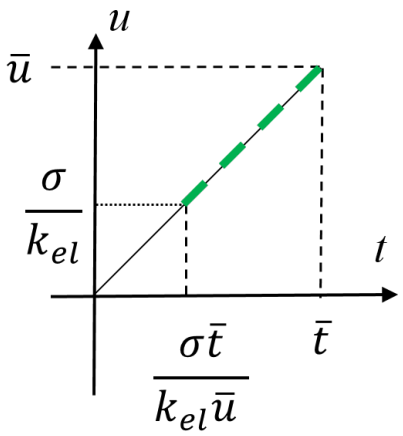

FIGURE 4. The plastic irreversible phase one of the loading history in terms of the imposed displacement u vs time t.

of time, and therefore, it remains negative,

$$\lambda_{cy} < 0, \qquad \forall t \in [\frac{\sigma \bar{t}}{k_{el}\bar{u}}, \bar{t}]. \tag{4.40}$$

This means that the KKT condition (3.30) can be satisfied only setting to zero the increment $\Delta\lambda_c$ and therefore also the values of the plastic multiplier in compression for all the times in this part of the loading history,

$$\lambda_c\,(t) = 0, \qquad \forall t \in [\frac{\sigma \bar{t}}{k_{el}\bar{u}}, \bar{t}]. \tag{4.41}$$

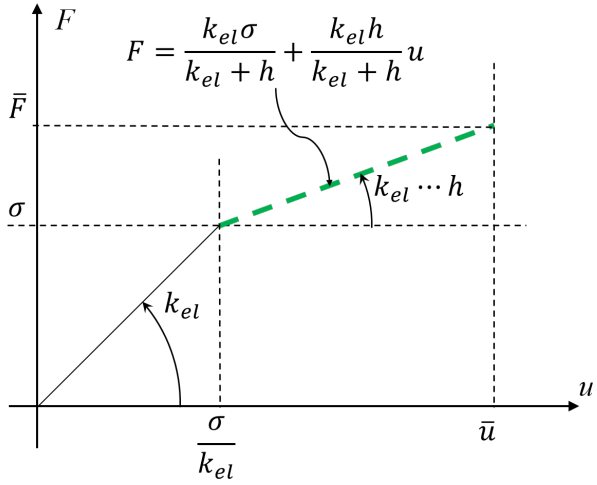

FIGURE 5. Plastic irreversible phase one response is highlighted with the green-dashed line. We plot the reaction force F vs the imposed displacement u.

Besides, the yielding tension from (3.22) and (4.41) becomes positive,

$$\lambda_{ty} = \frac{k_{el}u - \sigma}{k_{el}+h} > 0, \qquad \forall t \in [\frac{\sigma \bar{t}}{k_{el}\bar{u}}, \bar{t}],$$

and the KKT condition (3.29) is satisfied in terms of the plastic multiplier in tension by

$$\lambda_t(t) = \lambda_{ty} = \frac{k_{el}u - \sigma}{k_{el}+h}, \qquad \forall t \in [\frac{\sigma \bar{t}}{k_{el}\bar{u}}, \bar{t}]. \tag{4.42}$$

The spring response, according to (3.26), (4.41) and (4.42), is as follows,

$$k_{el}\left(u - \lambda_t(t) + \lambda_c(t)\right) = k_{el}\left(u - \frac{k_{el}u - \sigma}{k_{el}+h}\right) = F, \qquad \forall t \in [\frac{\sigma \bar{t}}{k_{el}\bar{u}}, \bar{t}],$$

that means

$$F = k_{el}\left(\frac{hu + \sigma}{k_{el}+h}\right) = \frac{k_{el}}{k_{el}+h}\sigma + \frac{hk_{el}}{k_{el}+h}u, \qquad \forall t \in [\frac{\sigma \bar{t}}{k_{el}\bar{u}}, \bar{t}], \tag{4.43}$$

that is a spring with a residual (with no displacement $u = 0$) force equal to

$$\frac{k_{el}}{k_{el}+h}\sigma,$$

and a stiffness

$$\frac{hk_{el}}{k_{el}+h}, \tag{4.44}$$

that is the equivalent stiffness of the series of two springs, one with stiffness k_{el} and one with stiffness h. The response is therefore represented in Fig. 5. As a matter of fact, from (4.42) the final value of the plastic multiplier in tension is

$$\lambda_t(t = \bar{t}) = \frac{k_{el}\bar{u} - \sigma}{k_{el}+h} > 0 \tag{4.45}$$

and from (4.43), the final value of the reaction force is

$$\hat{F}\left(t=\bar{t}\right)=\overline{F}=k_{el}\frac{\sigma+h\overline{u}}{k_{el}+h}. \tag{4.46}$$

In this phase, the dissipation energy is derived by the insertion of (4.41) and (4.42) into (3.17).

If, in an arbitrary moment $t=\widetilde{t}$ at $u=u\left(t=\widetilde{t}\right)=\widetilde{u}$ of this plastic irreversible phase, we change the sign of the loading velocity $\dot{u}$, then the KKT conditions (3.29) and (3.30) would both be satisfied setting to zero the increments $\Delta\lambda_t$ and $\Delta\lambda_c$, and therefore, the value of the plastic multiplier in compression would be still the same of that already calculated in (4.41)

$$\lambda_c\left(t\right)=\widetilde{\lambda}_c=0, \qquad \forall t>\widetilde{t},$$

and that in tension would be from (4.42)

$$\lambda_t\left(t\right)=\widetilde{\lambda}_t=\frac{k_{el}\widetilde{u}-\sigma}{k_{el}+h}, \qquad \forall t>\widetilde{t},$$

and therefore the response would be

$$k_{el}\left(u-\widetilde{\lambda}_t+\widetilde{\lambda}_c\right)=k_{el}\left(u-\frac{k_{el}\widetilde{u}-\sigma}{k_{el}+h}\right)=F, \qquad \forall t>\widetilde{t},$$

that is different from that calculated in (4.43). In particular, the tangent stiffness would be k_{el} and not the series reported in (4.44). This irreversible behavior justifies the name "irreversible" of this phase of the loading history.

4.4. **The elastic reversible phase two.** In the third part of the loading history, the displacement u is imposed to evolve according to Fig. 1. Thus, it changes the sign of its time derivative $\dot{u}$, and therefore, the spring is in an unloading phase. Besides, in this elastic reversible phase two, it is limited to be

$$\overline{\bar{u}}=\bar{u}-2\frac{\sigma}{k_{el}}<u<\bar{u}, \qquad \forall t\in[\bar{t},\bar{t}+2\frac{\sigma\bar{t}}{k_{el}\bar{u}}], \tag{4.47}$$

and it is graphically represented in Fig. 6. Thus, the yielding tension is from (3.22) a decreasing function of time, and therefore, it is always lower than the final value $\lambda_t\left(t=\bar{t}\right)$ of the plastic multiplier in tension calculated in (4.45), that is the last one taken during the previous plastic irreversible one part of the loading history,

$$\lambda_{ty}<\lambda_t\left(t=\bar{t}\right)=\frac{k_{el}\bar{u}-\sigma}{k_{el}+h}, \qquad \forall t\in[\bar{t},\bar{t}+2\frac{\sigma\bar{t}}{k_{el}\bar{u}}]. \tag{4.48}$$

The KKT condition (3.29) is satisfied only setting to zero the increment $\Delta\lambda_t$, and therefore, also keeping constant the values of the plastic multiplier in tension for all the times in this part of the loading history,

$$\lambda_t\left(t\right)=\frac{k_{el}\bar{u}-\sigma}{k_{el}+h}, \qquad \forall t\in[\bar{t},\bar{t}+2\frac{\sigma\bar{t}}{k_{el}\bar{u}}]. \tag{4.49}$$

Besides, the yielding compression is from (3.23) an increasing function of time,

$$\lambda_{cy}=\frac{k_{el}\bar{u}-\sigma}{k_{el}+h}-\frac{k_{el}u+\sigma}{k_{el}+h}=\frac{k_{el}\left(\bar{u}-u\right)-2\sigma}{k_{el}+h}<0, \qquad \forall t\in[\bar{t},\bar{t}+2\frac{\sigma\bar{t}}{k_{el}\bar{u}}], \tag{4.50}$$

but it remains negative in the prescribed range (4.47) of the present third phase of the loading history so that we still have that the KKT condition (3.30) can be satisfied only by setting to

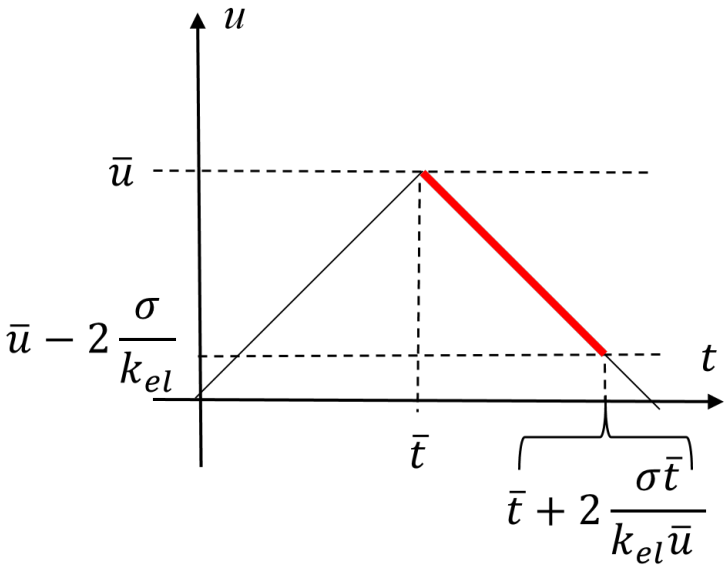

FIGURE 6. The elastic reversible phase two of the loading history in terms of the imposed displacement u vs time t.

zero the increment $\Delta\lambda_c$, and therefore, also the values of the plastic multiplier in compression for all the times in this part of the loading history,

$$\lambda_c(t) = 0, \qquad \forall t \in [\bar{t}, \bar{t} + 2\frac{\sigma\bar{t}}{k_{el}\bar{u}}]. \tag{4.51}$$

The spring response is, according to (3.26), (4.49) and (4.51), as follows,

$$k_{el}\left(u - \lambda_t(t) + \lambda_c(t)\right) = k_{el}\left(u - \frac{k_{el}\bar{u} - \sigma}{k_{el} + h}\right) = F = \hat{F}(t), \qquad \forall t \in [\bar{t}, \bar{t} + 2\frac{\sigma\bar{t}}{k_{el}\bar{u}}], \tag{4.52}$$

that is a spring with a residual (with no displacement $u = 0$) force equal to

$$k_{el}\left(\frac{\sigma - k_{el}\bar{u}}{k_{el} + h}\right),$$

and the same initial elastic stiffness

$$k_{el}.$$

The two plastic multipliers do not change their values, and this justifies calling elastic this part of the loading history. The response is therefore represented according to Fig. 7. As a matter of fact the final value of the reaction force is from (4.52)

$$F = \hat{F}\left(t = \bar{t} + 2\frac{\sigma\bar{t}}{k_{el}\bar{u}}\right) = \overline{\overline{F}} = \overline{F} - 2\sigma.$$

If, in an arbitrary moment of this elastic reversible phase, we change the sign of the loading velocity $\dot{u}$, then the KKT conditions (3.29) and (3.30) will be both satisfied with the same constant values of plastic multipliers (4.49) and (4.51), and therefore, the response is the same as calculated in (4.52) and graphically reported in Fig. 7. This reversible behavior justifies the name "reversible" for this phase of the loading history.

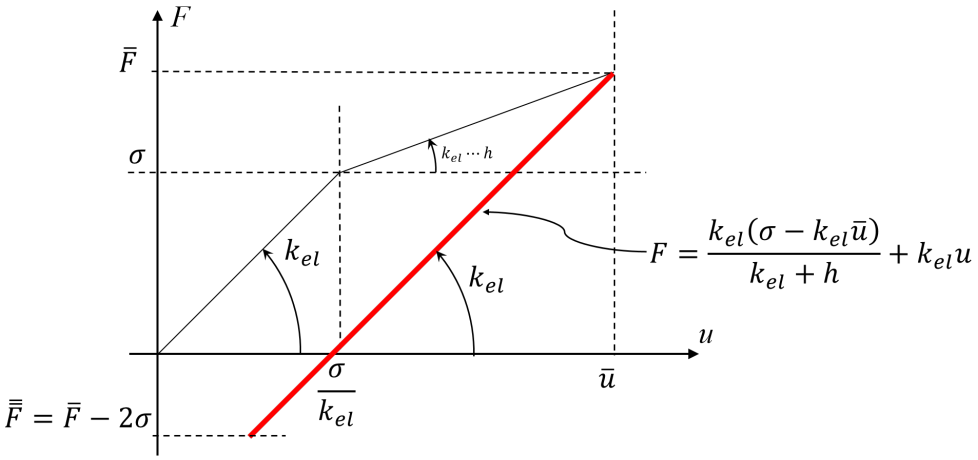

FIGURE 7. Elastic reversible phase two response is highlighted with the red-thick line. We plot the reaction force F vs the imposed displacement u.

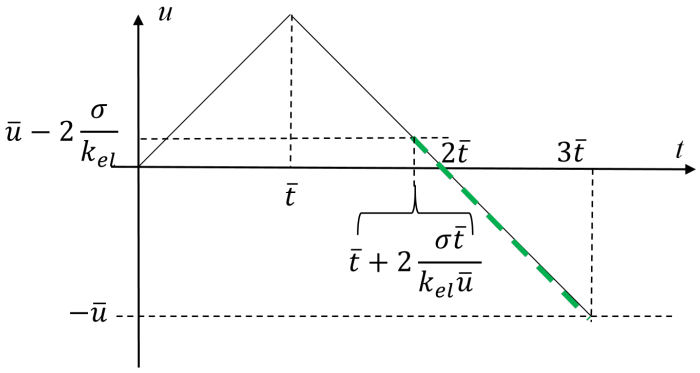

FIGURE 8. The plastic irreversible phase two of the loading history in terms of the imposed displacement u vs time t.

4.5. **The plastic irreversible phase two.** In the fourth part of loading history, the displacement u is imposed to evolve according to Fig. 1. Besides, in this plastic irreversible phase two, the spring is still in an unloading phase and it is limited to be

$$-\bar{u} < u < \bar{u} - 2\frac{\sigma}{k_{el}}, \qquad \forall t \in [\bar{t} + 2\frac{\sigma\bar{t}}{k_{el}\bar{u}}, 3\bar{t}], \tag{4.53}$$

and it is graphically represented in Fig. 8.

The yielding tension is from (3.22) again a decreasing function of time (because the displacement u is a decreasing function of time), and therefore, it continues to be always lower than the value (that was constant in the previous stage) of the plastic multiplier λ_t in (4.49),

$$\lambda_{ty} < \lambda_t\left(t = \bar{t} + 2\frac{\sigma\bar{t}}{k_{el}\bar{u}}\right) = \frac{k_{el}\bar{u} - \sigma}{k_{el} + h}, \qquad \forall t \in [\bar{t} + 2k_{el}\bar{u}, 3\bar{t}]. \tag{4.54}$$

Thus, the KKT condition is satisfied only setting to zero the increment $\Delta\lambda_t$, and therefore also the values of the plastic multiplier in tension for all the times in this part of the loading history,

$$\lambda_t(t) = \frac{k_{el}\bar{u} - \sigma}{k_{el} + h}, \qquad \forall t \in [\bar{t} + 2\frac{\sigma\bar{t}}{k_{el}\bar{u}}, 3\bar{t}]. \tag{4.55}$$

Besides, the yielding compression is from (3.23) an increasing function of time (because the displacement u is a decreasing function of time),

$$\lambda_{cy}(t) = \frac{k_{el}\bar{u} - \sigma}{k_{el} + h} - \frac{k_{el}u + \sigma}{k_{el} + h} = \frac{k_{el}(\bar{u} - u) - 2\sigma}{k_{el} + h} > \lambda_c\left(\bar{t} + 2\frac{\sigma\bar{t}}{k_{el}\bar{u}}\right) = 0, \qquad \forall t \in [\bar{t} + 2\frac{\sigma\bar{t}}{k_{el}\bar{u}}, 3\bar{t}], \tag{4.56}$$

but now it is positive (and therefore because of (4.51) greater than the plastic multiplier in compression in the previous stage) in the prescribed range (4.53) of the fourth part of the loading history so that the KKT condition condition (3.30) is satisfied by,

$$\lambda_c(t) = \lambda_{cy}(t) = \frac{k_{el}(\bar{u} - u) - 2\sigma}{k_{el} + h}, \qquad \forall t \in [\bar{t} + 2\frac{\sigma\bar{t}}{k_{el}\bar{u}}, 3\bar{t}]. \tag{4.57}$$

The spring response is, according to (3.26), (4.55) and (4.57), as follows,

$$k_{el}(u - \lambda_t(t) + \lambda_c(t)) = k_{el}\left(u - \frac{k_{el}\bar{u} - \sigma}{k_{el} + h} + \frac{k_{el}(\bar{u} - u) - 2\sigma}{k_{el} + h}\right) = F,$$

that means

$$\frac{k_{el}h}{k_{el} + h}u - k_{el}\frac{\sigma}{k_{el} + h} = \hat{F}(t), \qquad \forall t \in [\bar{t} + 2\frac{\sigma\bar{t}}{k_{el}\bar{u}}, 3\bar{t}], \tag{4.58}$$

that is a spring with a residual (with no displacement $u = 0$) force equal to

$$-k_{el}\frac{\sigma}{k_{el} + h},$$

and a stiffness (4.44), that is the equivalent stiffness of the series of two springs, one with stiffness k_{el} and one with stiffness h. The response is therefore represented according to Fig. 9.

As a matter of facts, from (4.57) the final value of plastic multiplier in compression is

$$\lambda_c(t = 3\bar{t}) = \frac{k_{el}(\bar{u} - u(t = 3\bar{t})) - 2\sigma}{k_{el} + h} = \frac{k_{el}(\bar{u} - (-\bar{u})) - 2\sigma}{k_{el} + h} = 2\frac{k_{el}\bar{u} - \sigma}{k_{el} + h}, \tag{4.59}$$

and from (4.58) the final value of the reaction response is

$$\hat{F}(t = 3\bar{t}) = \frac{k_{el}h}{k_{el} + h}u(t = 3\bar{t}) - k_{el}\frac{\sigma}{k_{el} + h} = -\frac{k_{el}h}{k_{el} + h}\bar{u} - k_{el}\frac{\sigma}{k_{el} + h} = -k_{el}\frac{\sigma + h\bar{u}}{k_{el} + h} = -\overline{F}.$$

If, in an arbitrary moment $t = \widetilde{t}$ at $u = u(t = \widetilde{t}) = \widetilde{u}$ of this plastic irreversible phase, we change the sign of the loading velocity $\dot{u}$ then the KKT conditions (3.29) and (3.30) would both be satisfied setting to zero the increments $\Delta\lambda_t$ and $\Delta\lambda_c$, and therefore, the value of the plastic multiplier in tension would be still the same of that already calculated in (4.55)

$$\lambda_t(t) = \widetilde{\lambda}_t = \frac{k_{el}\bar{u} - \sigma}{k_{el} + h}, \qquad \forall t > \widetilde{t},$$

and that in compression would be from (4.57)

$$\lambda_c(t) = \widetilde{\lambda}_c = \frac{k_{el}(\bar{u} - \widetilde{u}) - 2\sigma}{k_{el} + h}, \qquad \forall t > \widetilde{t},$$

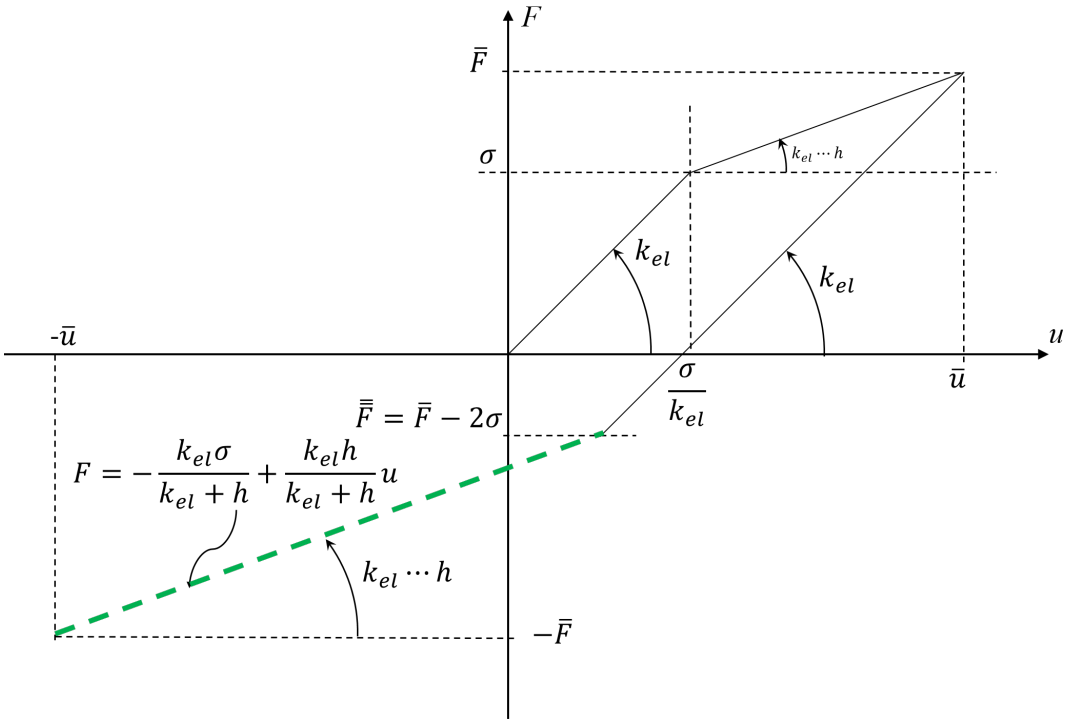

FIGURE 9. Plastic irreversible phase two response is highlighted with the green-dashed line. We plot the reaction force F vs the imposed displacement u.

and therefore, the response would be

$$k_{el}\left(u-\widetilde{\lambda}_t+\widetilde{\lambda}_c\right)=k_{el}\left(u-\frac{k_{el}\widetilde{u}-\sigma}{k_{el}+h}+\frac{k_{el}\left(\bar{u}-\widetilde{u}\right)-2\sigma}{k_{el}+h}\right)=k_{el}\left(u-\frac{2k_{el}\widetilde{u}-k_{el}\bar{u}+\sigma}{k_{el}+h}\right)$$
$$=F,\qquad \forall t>\widetilde{t},$$

that is different from that calculated in (4.58). In particular the tangent stiffness would be k_{el} and not the series reported in (4.44). This irreversible behavior justifies the name "irreversible" of this phase of the loading history.

4.6. **The elastic reversible phase three.** In the fifth part of the loading history, the displacement u is imposed to evolve according to Fig. 1. Thus, it changes the sign of its time derivative $\dot{u}$ and therefore the spring is again in a loading phase. Besides, in this elastic reversible phase three it is limited to be

$$-\bar{u}<u<-\bar{u}+2\frac{\sigma}{k_{el}},\qquad \forall t\in[3\bar{t},3\bar{t}+2\frac{\sigma\bar{t}}{k_{el}\bar{u}}], \tag{4.60}$$

and it is graphically represented in Fig. 10. The yielding compression is from (3.23) a decreasing function of time (because the displacement u is an increasing function of time) so that it remains

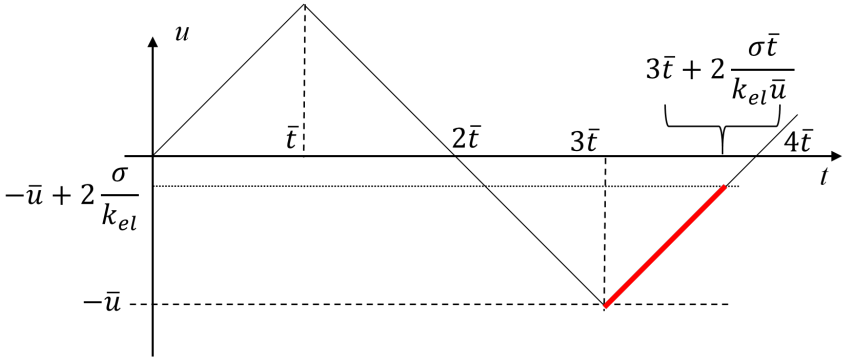

FIGURE 10. The elastic reversible phase three of the loading history in terms of the imposed displacement u vs time t.

always lower than the last value (4.59) of the previous stage of the loading history,

$$\lambda_{cy}(t) < \lambda_{cy}(t=3\bar{t}) = \lambda_c(t=3\bar{t}) = 2\frac{k_{el}\bar{u}-\sigma}{k_{el}+h}, \qquad \forall t \in [3\bar{t}, 3\bar{t}+2\frac{\sigma\bar{t}}{k_{el}\bar{u}}].$$

Thus, the KKT condition (3.30) for the plastic multiplier in compression is satisfied only setting to zero the increment $\Delta\lambda_c$ and therefore it yields also constant the function of the plastic multiplier in compression for all the times in this part of the loading history,

$$\lambda_c(t) = 2\frac{k_{el}\bar{u}-\sigma}{k_{el}+h}, \qquad \forall t \in [3\bar{t}, 3\bar{t}+2\frac{\sigma\bar{t}}{k_{el}\bar{u}}]. \tag{4.61}$$

Besides, the yielding tension (because the displacement u is an increasing function of time) is an increasing function of time but still lower than the previous value $\lambda_t(t=3\bar{t})$ of the plastic multiplier in tension

$$\lambda_{ty} = 2\frac{k_{el}\bar{u}-\sigma}{k_{el}+h} + \frac{k_{el}u-\sigma}{k_{el}+h} < \lambda_t(t=3\bar{t}) = \frac{k_{el}\bar{u}-\sigma}{k_{el}+h}, \qquad \forall t \in [3\bar{t}, 3\bar{t}+2\frac{\sigma\bar{t}}{k_{el}\bar{u}}].$$

Thus, the KKT condition (3.29) for the plastic multiplier in tension is satisfied only setting to zero the increment $\Delta\lambda_t$ and therefore it yields also constant the function of the plastic multiplier in tension for all the times in this part of the loading history,

$$\lambda_t(t) = \lambda_t(t=3\bar{t}) = \frac{k_{el}\bar{u}-\sigma}{k_{el}+h}, \qquad \forall t \in [3\bar{t}, 3\bar{t}+2\frac{\sigma\bar{t}}{k_{el}\bar{u}}]. \tag{4.62}$$

From (4.61) and (4.62) we have that plastic multipliers are constant and this justifies to call elastic the present fifth phase of the loading history. The spring response is, according to (3.26), (4.61) and (4.62), as follows,

$$k_{el}(u-\lambda_t(t)+\lambda_c(t)) = k_{el}\left(u - \frac{k_{el}\bar{u}-\sigma}{k_{el}+h} + 2\frac{k_{el}\bar{u}-\sigma}{k_{el}+h}\right) = F,$$

that means

$$k_{el}u + k_{el}\left(\frac{k_{el}\bar{u}-\sigma}{k_{el}+h}\right) = \hat{F}(t), \qquad \forall t \in [3\bar{t}, 3\bar{t}+2\frac{\sigma\bar{t}}{k_{el}\bar{u}}], \tag{4.63}$$

that is a spring with a residual (with no displacement $u=0$) force equal to

$$k_{el}\left(\frac{k_{el}\bar{u}-\sigma}{k_{el}+h}\right),$$

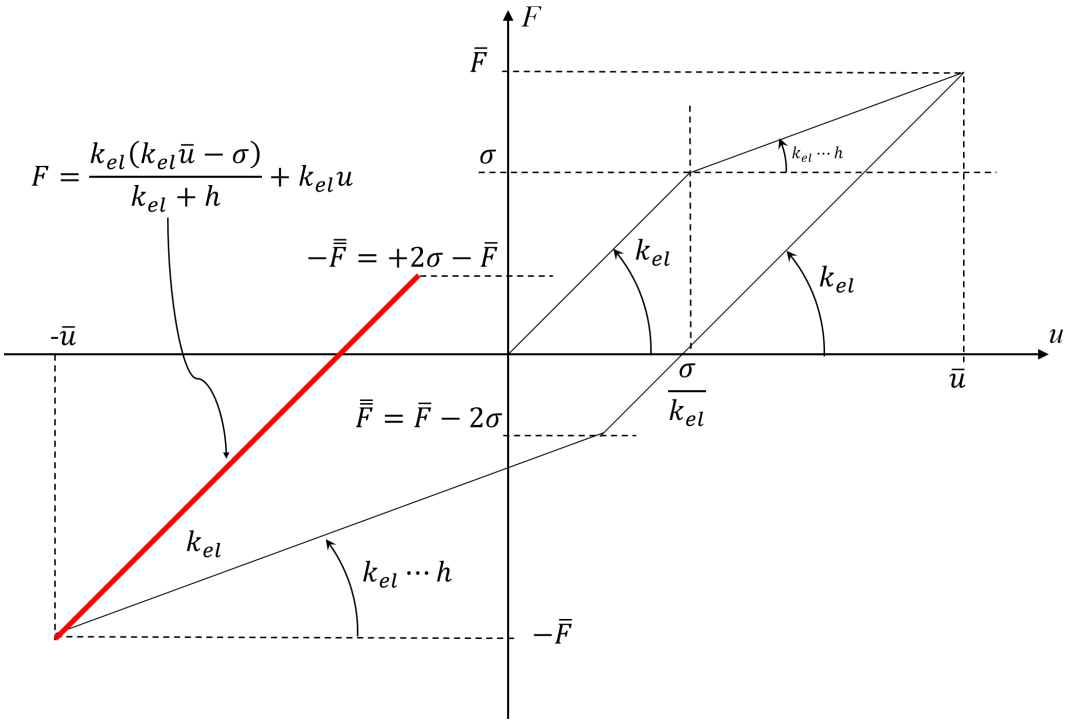

FIGURE 11. Elastic reversible phase three response is highlighted with the red-thick line. We plot the reaction force F vs the imposed displacement u.

and a stiffness

$$k_{el}.$$

The response is therefore graphically represented in Fig. 11.

As a matter of facts the final value of the reaction force is from (4.63)

$$\hat{F}\left(t = 3\bar{t} + 2\frac{\sigma\bar{t}}{k_{el}\bar{u}}\right) = k_{el}\left(-\bar{u} + 2\frac{\sigma}{k_{el}}\right) + k_{el}\left(\frac{k_{el}\bar{u} - \sigma}{k_{el} + h}\right) = 2\sigma - k_{el}\frac{h\bar{u} + \sigma}{k_{el} + h} = 2\sigma - \overline{F} = -\overline{\overline{F}}.$$

If, in an arbitrary moment of this elastic reversible phase we change the sign of the loading velocity $\dot{u}$ then the KKT conditions (3.29) and (3.30) will be both satisfied with the same constant values of plastic multipliers (4.61) and (4.62) and therefore the response is the same as calculated in (4.63) and graphically reported in Fig. 11. This reversible behavior justifies the name "reversible" for this phase of the loading history.

4.7. **The plastic irreversible phase three.** In the sixth part of the loading history the displacement u is imposed to evolve according to Fig. 1. Besides, in this plastic irreversible phase three, the spring is still in a loading phase and it is limited to be

$$-\bar{u} + 2\frac{\sigma}{k_{el}} < u < \bar{u}, \qquad \forall t \in [3\bar{t} + 2\frac{\sigma\bar{t}}{k_{el}\bar{u}}, 5\bar{t}], \tag{4.64}$$

and it is graphically represented in Fig. 12. The yielding compression is from (3.23) again a decreasing function of time (because the displacement u is still an increasing function of

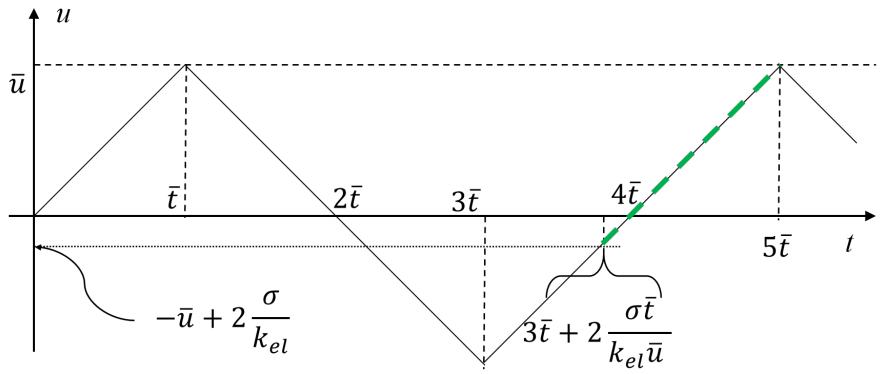

FIGURE 12. The plastic irreversible phase three of the loading history in terms of the imposed displacement u vs time t.

time), and therefore it is always lower than the final value in (4.61) of the plastic multiplier in compression of the previous part of the loading history

$$\lambda_{cy} < \lambda_c\left(t = 3\bar{t} + 2\frac{\sigma\bar{t}}{k_{el}\bar{u}}\right) = 2\frac{k_{el}\bar{u} - \sigma}{k_{el} + h}, \qquad \forall t \in [3\bar{t} + 2\frac{\sigma\bar{t}}{k_{el}\bar{u}}, 5\bar{t}]. \tag{4.65}$$

Thus, the KKT condition (3.30) is satisfied only setting to zero the increment $\Delta\lambda_c$ and therefore it yields also constant the function of the plastic multiplier in compression for all the times in this part of the loading history,

$$\lambda_c(t) = 2\frac{k_{el}\bar{u} - \sigma}{k_{el} + h}, \qquad \forall t \in [3\bar{t} + 2\frac{\sigma\bar{t}}{k_{el}\bar{u}}, 5\bar{t}]. \tag{4.66}$$

Besides, the yielding tension is from (3.22) an increasing function of time (because the displacement u is still an increasing function of time),

$$\lambda_{ty}(t) = 2\frac{k_{el}\bar{u} - \sigma}{k_{el} + h} + \frac{k_{el}u - \sigma}{k_{el} + h} = \frac{k_{el}(2\bar{u} + u) - 3\sigma}{k_{el} + h} > \frac{k_{el}\bar{u} - \sigma}{k_{el} + h} = \lambda_t(t = 3\bar{t}), \quad \forall t \in [3\bar{t} + 2\frac{\sigma\bar{t}}{k_{el}\bar{u}}, 5\bar{t}]. \tag{4.67}$$

It is greater than, because of (4.62), the value of the plastic multiplier in tension $\lambda_t(t = 3\bar{t})$ at the previous last instant of time of the fifth part of the loading history. Thus, the KKT condition (3.29) is satisfied by,

$$\lambda_t(t) = \lambda_{ty}(t) = \frac{k_{el}(2\bar{u} + u) - 3\sigma}{k_{el} + h}, \qquad \forall t \in [3\bar{t} + 2\frac{\sigma\bar{t}}{k_{el}\bar{u}}, 5\bar{t}]. \tag{4.68}$$

The spring response is, according to (3.26), (4.66) and (4.68), as follows,

$$F = k_{el}(u - \lambda_t(t) + \lambda_c(t)) = k_{el}\left(u - \frac{k_{el}(2\bar{u} + u) - 3\sigma}{k_{el} + h} + 2\frac{k_{el}\bar{u} - \sigma}{k_{el} + h}\right),$$

that means

$$\frac{k_{el}h}{k_{el} + h}u + k_{el}\frac{\sigma}{k_{el} + h} = \hat{F}(t), \qquad \forall t \in [3\bar{t} + 2\frac{\sigma\bar{t}}{k_{el}\bar{u}}, 5\bar{t}], \tag{4.69}$$

that is a spring with a residual (with no displacement $u = 0$) force equal to

$$k_{el}\frac{\sigma}{k_{el} + h},$$

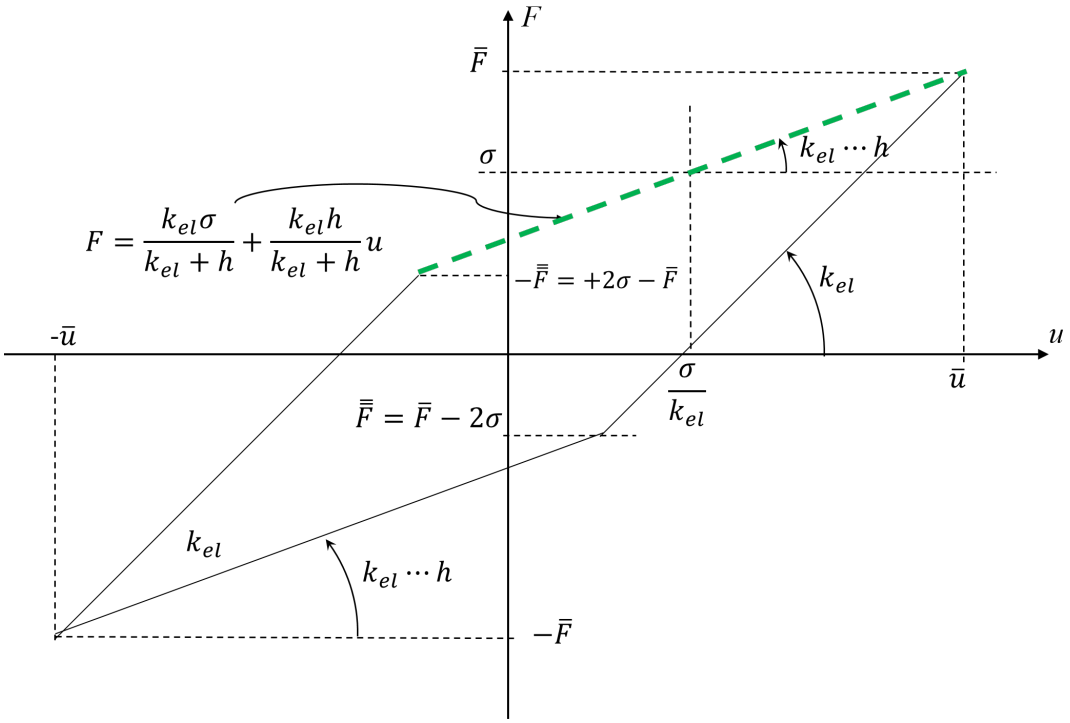

FIGURE 13. Plastic irreversible phase three response is highlighted with the green-dashed line. We plot the reaction force F vs the imposed displacement u.

and a stiffness (4.44), that is the equivalent stiffness of the series of two springs, one with stiffness k_{el} and one with stiffness h. The response is therefore represented according to Fig. 13.

As a matter of facts, from (4.68) the final value of plastic multiplier in tension is

$$\lambda_t\left(t=5\bar{t}\right)=\frac{k_{el}\left(2\bar{u}+u\left(t=5\bar{t}\right)\right)-3\sigma}{k_{el}+h}=\frac{k_{el}\left(2\bar{u}+\bar{u}\right)-3\sigma}{k_{el}+h}=3\frac{k_{el}\bar{u}-\sigma}{k_{el}+h} \tag{4.70}$$

and from (4.69) the final value of the reaction response is

$$\hat{F}\left(t=5\bar{t}\right)=\frac{k_{el}h}{k_{el}+h}u\left(t=5\bar{t}\right)+k_{el}\frac{\sigma}{k_{el}+h}=\frac{k_{el}h}{k_{el}+h}\bar{u}+k_{el}\frac{\sigma}{k_{el}+h}=k_{el}\frac{\sigma+h\bar{u}}{k_{el}+h}=\bar{F}.$$

If, in an arbitrary moment $t=\widetilde{t}$ at $u=u\left(t=\widetilde{t}\right)=\widetilde{u}$ of this plastic irreversible phase, we change the sign of the loading velocity $\dot{u}$ then the KKT conditions (3.29) and (3.30) would both be satisfied setting to zero the increments $\Delta\lambda_t$ and $\Delta\lambda_c$ and therefore the value of the plastic multiplier in compression would be still the same of that already calculated in (4.66)

$$\lambda_c\left(t\right)=\widetilde{\lambda}_c=2\frac{k_{el}\bar{u}-\sigma}{k_{el}+h},\qquad\forall t>\widetilde{t},$$

and that in tension would be from (4.68)

$$\lambda_t\left(t\right)=\widetilde{\lambda}_t=\frac{k_{el}\left(2\bar{u}+\widetilde{u}\right)-3\sigma}{k_{el}+h},\qquad\forall t>\widetilde{t},$$

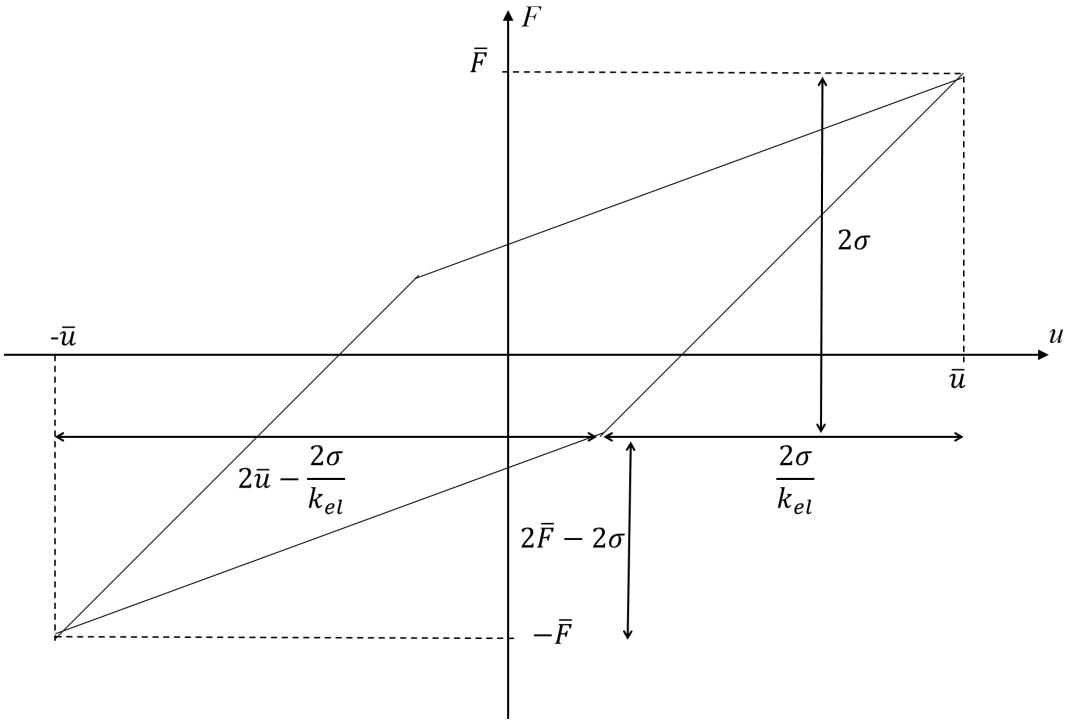

FIGURE 14. Measures for calculating the dissipated area of the hysteretic loop.

and therefore the response would be

$$k_{el}\left(u-\widetilde{\lambda}_t+\widetilde{\lambda}_c\right)=k_{el}\left(u-\frac{k_{el}\left(2\bar{u}+\widetilde{u}\right)-3\sigma}{k_{el}+h}+2\frac{k_{el}\bar{u}-\sigma}{k_{el}+h}\right)=k_{el}\left(u-\frac{k_{el}\widetilde{u}-\sigma}{k_{el}+h}\right)$$
$$=F, \qquad \forall t>\widetilde{t},$$

that is different from that calculated in (4.69). In particular the tangent stiffness would be k_{el} and not the series reported in (4.44). This irreversible behavior justifies the name "irreversible" of this phase of the loading history.

4.8. **Dissipated energy per unit cycle.** The dissipated energy per unit cycle can be calculated into two ways. The first is simply by measuring the area within the hysteretic loop

The area of the external rectangle R_e is

$$R_e = 2\overline{F}2\sigma = 4\sigma\overline{F}.$$

The areas A above and bottom the hysteretic area H_y are the same so that

$$H_y = R_e - 2A = R_e - 2\left(R_s + T_l + T_a\right).$$

Such areas are composed by two triangles and one small rectangle R_s with area

$$R_s = \left(2\overline{F} - 2\sigma\right)\frac{2\sigma}{k_{el}}.$$

Let us consider the below area. The below triangle T_l is

$$T_l = \frac{1}{2}\left(2\overline{u} - \frac{2\sigma}{k_{el}}\right)\left(2\overline{F} - 2\sigma\right),$$

the above triangle T_a is

$$T_a = \frac{1}{2}\left(\frac{2\sigma}{k_{el}}\right)(2\sigma).$$

Combining the previous equations, we obtain

$$H_y = 4\sigma\overline{F} - 2\left[\left(2\overline{F} - 2\sigma\right)\frac{2\sigma}{k_{el}} + \frac{1}{2}\left(2\overline{u} - \frac{2\sigma}{k_{el}}\right)\left(2\overline{F} - 2\sigma\right) + \frac{1}{2}\left(\frac{2\sigma}{k_{el}}\right)(2\sigma)\right] = 4\sigma\left(\overline{u} - \frac{\overline{F}}{k_{el}}\right),$$

that, from (4.46) we have

$$H_y = 4\sigma\left(\frac{k_{el}\overline{u} - \sigma}{k_{el} + h}\right).$$

Another way is to calculate the dissipation energy (3.17) at the displacement within the plastic irreversible phase three (4.64)

$$u = \frac{\sigma}{k_{el}}.$$

From (4.66) we have

$$\lambda_c = 2\frac{k_{el}\bar{u} - \sigma}{k_{el} + h},$$

and from (4.68)

$$\lambda_t = \frac{k_{el}\left(2\bar{u} + \frac{\sigma}{k_{el}}\right) - 3\sigma}{k_{el} + h},$$

that implies that the two accumulations are the same and the dissipation(3.17) is

$$W = 4\sigma\frac{k_{el}\bar{u} - \sigma}{k_{el} + h} = H_y,$$

that is consistent with the area H_y of the hysteretic cycle.

4.9. **Evolution of the plastic multipliers.** In the previous subsections, we have calculated analytically, among the reaction force evolution F, also both the plastic multipliers λ_t and λ_c. Besides, a graphical evolution of the hysteretic loop is also furnished. In this subsection, we want to give an analogous graphical evolution also of the plastic multipliers λ_t and λ_c and, because of (2.5) also of the plastic displacement u_{pl}. In Fig. 15, we show such an evolution versus time. We observe that for elastic phases both λ_t and λ_c are constant. As a consequence, also the plastic displacement u_{pl} is constant. Besides, the investigated plastic phases are 3. During the first and the third plastic phase, only λ_c is constant, and λ_t linearly evolves. During the second plastic phase only λ_t is constant, and λ_c linearly evolves. As a consequence, during the first and the third plastic phase, the plastic displacement u_{pl} linearly increases, and during the second plastic phase, it linearly decreases.

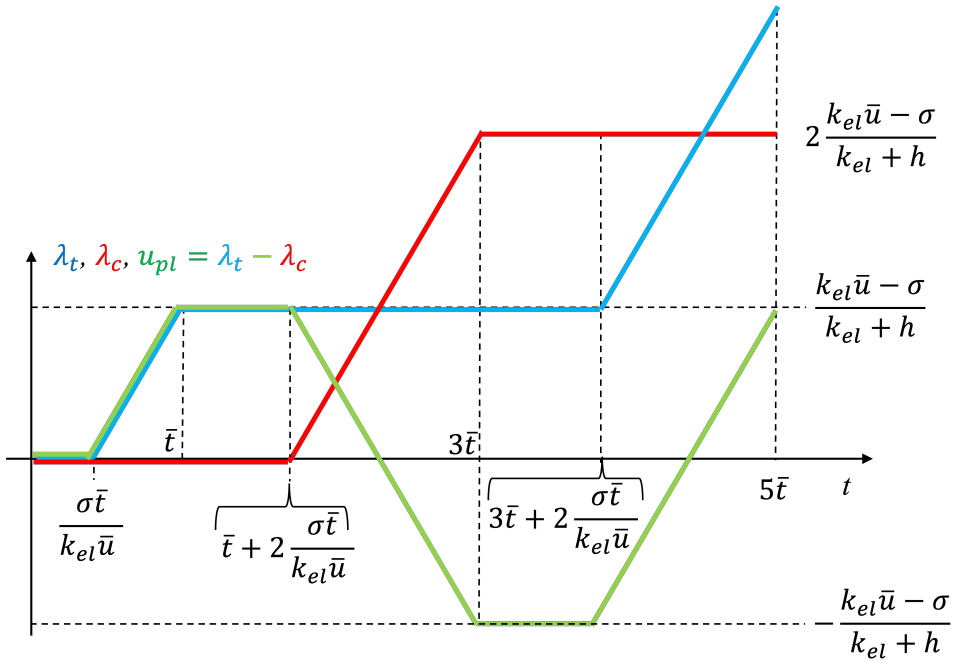

FIGURE 15. Evolutions of the plastic multipliers λ_t (blue line) and λ_c (red line) and of plastic displacement $u_{pl} = \lambda_t - \lambda_c$ (green line) are shown as a function of time.

5. CONCLUSION

A hemivariational derivation of the linear hardening spring is derived analytically. Three kinematical descriptors have been used, i.e. one displacement u and two plastic multipliers λ_t and λ_c. The two plastic multipliers are interpreted as the plastic displacement accumulation in tension and in compression, and the plastic displacement u_{pl} is therefore simply assumed to be the difference $u_{pl} = \lambda_t - \lambda_c$ between the two plastic multipliers. On the one hand, variation of displacement δu is assumed to be arbitrary. On the other hand, mono-lateral constraints $\dot{\lambda}_t \geq 0$ and $\dot{\lambda}_c \geq 0$ are assumed on both the plastic multipliers, i.e. their variations $\delta\lambda_t$ and $\delta\lambda_c$ can only be positive $\delta\lambda_t \geq 0$ and $\delta\lambda_c \geq 0$ because they can only increase with time. This is the reason why a hemivariational principle has been used. The last assumptions concern only the functional form of the elastic energy U, that is quadratic with respect to the elastic part $u_{el} = u - u_{pl}$ of the displacement function, of the dissipation energy W, that is assumed to be quadratic with respect to the plastic displacement u_{pl} and on the external energy U^{ext}, that is assumed to be linear with the displacement u. Besides, the elastic energy is also assumed to be proportional with respect to the elastic stiffness k_{el}, the dissipation energy is assumed to be proportional to the hardening coefficient h, and the external energy is proportional to the dual of the displacement, that is the external force F. Thus, only two constitutive coefficients k_{el} and h have been assumed and no flow rules has been introduced. Models for linear hardening phenomena are present in the literature. These models are equivalent to the present one. However, in this approach, the generalization of the response is easier because it is connected only to the form of the dissipation energy. Thus, we finally observe that linearity of the hardening behaviour explored in this paper has been achieved by considering a quadratic term in

the dissipation energy (3.17). This has had the consequence of a linear evolution of the plastic multipliers with respect to the imposed displacement. Thus, adding higher order terms of plastic multipliers in the form of the dissipation energy would modify such a linear hardening behavior. For example, a quartic dissipation energy would imply a cubic hardening behavior.

REFERENCES

[1] B. E. Abali, W. H. Müller and F. dell'Isola: *Theory and computation of higher gradient elasticity theories based on action principles*, Archive of Applied Mechanics, **87** (2017), 1495–1510.

[2] I. Ahmad, H. Ahmad, P. Thounthong, Y. Chu and C. Cesarano: *Solution of multi-term time-fractional PDE models arising in mathematical biology and physics by local meshless method*, Symmetry, **12** (2020), Article ID: 1195.

[3] E. Aifantis: *Pattern formation in plasticity*, Internat. J. Engrg. Sci., **33** (1995), 2161–2178.

[4] J. Alibert, P. Seppecher and F. Dell'Isola: *Truss modular beams with deformation energy depending on higher displacement gradients*, Math. Mech. Solids, **8** (2003), 51–73

[5] A. Al-Jaser, C. Cesarano, B. Qaraad and L. Iambor: *Second-Order Damped Differential Equations with Superlinear Neutral Term: New Criteria for Oscillation*, Axioms, **13** (2024), Article ID: 234.

[6] U. Andreaus, P. Baragatti: *Fatigue crack growth, free vibrations, and breathing crack detection of aluminium alloy and steel beams*, J. Strain Anal. Eng. Des., **44** (2009), 595–608.

[7] E. Artioli, F. Auricchio and L. Veiga: *Generalized midpoint integration algorithms for J2 plasticity with linear hardening*, Int. J. Numer. Methods Eng., **72** (2007), 422–463.

[8] N. Auffray, F. Dell'Isola, V. Eremeyev, A. Madeo and G. Rosi: *Analytical continuum mechanics à la Hamilton–Piola least action principle for second gradient continua and capillary fluids*, Math. Mech. Solids, **20** (2015), 375–417.

[9] E. Barchiesi, A. Misra, L. Placidi and E. Turco: *Granular micromechanics-based identification of isotropic strain gradient parameters for elastic geometrically nonlinear deformations*, ZAMM Z. Angew. Math. Mech., **101** (11) (2021), Article ID: e202100059.

[10] M. Bragaglia, F. Lamastra, P. Russo, L. Vitiello, M. Rinaldi, F. Fabbrocino and F. Nanni: *A comparison of thermally conductive polyamide 6-boron nitride composites produced via additive layer manufacturing and compression molding*, Polym. Compos., **42** (2021), 2751–2765.

[11] M. Bragaglia, L. Paleari, F. Lamastra, D. Puglia, F. Fabbrocino and F. Nanni: *Graphene nanoplatelet, multiwall carbon nanotube, and hybrid multiwall carbon nanotube–graphene nanoplatelet epoxy nanocomposites as strain sensing coatings*, J. Reinf. Plast. Comp., **40** (2021), 632–643.

[12] M. Bragaglia, L. Paleari, F. Lamastra, P. Russo, F. Fabbrocino and F. Nanni: *Oleylamine functionalization of boron nitride nano-platelets for Polyamide-6 thermally conductive injection moulded composites*, J. Thermoplast. Compos. Mater., **36** (2023), 2862–2882.

[13] A. Caporale, R. Luciano and E. Sacco: *Micromechanical analysis of interfacial debonding in unidirectional fiber-reinforced composites*, Comput. Struct., **84** (2006), 2200–2211.

[14] A. Cauchy: *Sur l'èquilibre et le mouvement d'un système de points matèriels sollicitès par des forces d'attraction ou de rèpulsion mutuelle*, In: Oeuvres Complètes: Series 2. Cambridge Library Collection - Mathematics, Cambridge University Press, (2009) 227–252.

[15] A. Ciallella, I. Giorgio, E. Barchiesi, G. Alaimo, A. Cattenone, B. Smaniotto, A. Vintache, F. D'Annibale, F. Dell'Isola, F. Hild and Others: *A 3D pantographic metamaterial behaving as a mechanical shield: experimental and numerical evidence*, Mater. Des., **237** (2023), Article ID: 112554.

[16] L. Contrafatto, M. Cuomo and S. Gazzo: *A concrete homogenisation technique at meso-scale level accounting for damaging behaviour of cement paste and aggregates*, Comput. Struct., **173** (2016), 1–18.

[17] L. Contrafatto, M. Cuomo and L. Greco: *Meso-scale simulation of concrete multiaxial behaviour*, Eur. J. Environ. Civ. En., **21** (7–8) (2016), 896–911.

[18] F. Cornacchia, F. Fabbrocino, N. Fantuzzi, R. Luciano and R. Penna: *Analytical solution of cross-and angle-ply nano plates with strain gradient theory for linear vibrations and buckling*, Mech. Adv. Mater. Struct., **28** (2021), 1201–1215.

[19] M. Cuomo, L. Contrafatto and L. Greco: *A variational model based on isogeometric interpolation for the analysis of cracked bodies*, Int. J. Eng. Sci., **80** (2014), 173–188.

[20] C. D'Ambra, G. Lignola, A. Prota, F. Fabbrocino and E. Sacco: *FRCM strengthening of clay brick walls for out of plane loads*, Compos. B: Eng., **174** (2019), Article ID: 107050.

[21] F. De Angelis: *A comparative analysis of linear and nonlinear kinematic hardening rules in computational elastoplasticity*, Tech. Mech., **32** (2012), 164–173.

[22] G. Del Piero: *The variational structure of classical plasticity*, Math. Mech. Complex Syst., **6** (3) (2018), 137–180.

[23] F. Dell'Isola, S. Eugster, R. Fedele and P. Seppecher: *Second-gradient continua: From Lagrangian to Eulerian and back*, Math. Mech. Solids, **27** (2022), 2715–2750.

[24] F. Dell'Isola, I. Giorgio and U. Andreaus: *Elastic pantographic 2D lattices: a numerical analysis on static response and wave propagation*, Proc. Est. Acad. Sci., **64** (2015), 219–225.
[25] F. Dell'Isola, I. Giorgio, M. Pawlikowski and N. Rizzi: *Large deformations of planar extensible beams and pantographic lattices: heuristic homogenization, experimental and numerical examples of equilibrium*, Proc. R. Soc. A, **472** (2016), Article ID: 20150790.
[26] F. dell'Isola, M. Guarascio and K. Hutter: *A variational approach for the deformation of a saturated porous solid. A second-gradient theory extending Terzaghi's effective stress principle*, Arch. Appl. Mech., **70** (5) (2000), 323–337.
[27] F. Dell'Isola, A. Misra: *Principle of Virtual Work as Foundational Framework for Metamaterial Discovery and Rational Design*, C. R. Mecanique, **351** (2023), 1–25.
[28] F. Dell'Isola, A. Madeo and P. Seppecher: *Boundary conditions at fluid-permeable interfaces in porous media: A variational approach*, Int. J. Solids Struct., **46** (2009), 3150–3164.
[29] F. Dell'Isola, D. Steigmann: *A two-dimensional gradient-elasticity theory for woven fabrics*, J. Elast., **18** (2015), 113–125.
[30] C. Dharmawardhana, A. Misra, S. Aryal, P. Rulis and W. Ching: *Role of interatomic bonding in the mechanical anisotropy and interlayer cohesion of CSH crystals*, Cem. Concr. Res., **52** (2013), 123–130.
[31] V. Eremeyev, F. Dell'Isola, C. Boutin and D. Steigmann: *Linear pantographic sheets: existence and uniqueness of weak solutions*, J. Elast., **132** (2017), 175–196.
[32] S. Eugster, F. Dell'Isola, R. Fedele and P. Seppecher: *Piola transformations in second-gradient continua*, Mech. Res. Commun., **120** (2022), Article ID: 103836.
[33] F. Fabbrocino, G. Carpentieri: *Three-dimensional modeling of the wave dynamics of tensegrity lattices*, Compos. Struct., **173** (2017), 9–16.
[34] F. Fabbrocino, I. Farina: *Loading noise effects on the system identification of composite structures by dynamic tests with vibrodyne*, Compos. B: Eng., **115** (2017), 376–383.
[35] R. Fedele: *Piola's approach to the equilibrium problem for bodies with second gradient energies. Part I: First gradient theory and differential geometry*, Contin. Mech. Thermodyn., **34** (2022), 445–474.
[36] R. Fedele: *Third-gradient continua: nonstandard equilibrium equations and selection of work conjugate variables*, Math. Mech. Solids, **27** (2022), 2046–2072.
[37] R. Fedele, A. Ciani and F. Fiori: *X-ray microtomography under loading and 3D-volume digital image correlation A review*, Fundam. Inform., **135** (2014), 171–197.
[38] R. Fedele, M. Filippini and G. Maier: *Constitutive model calibration for railway wheel steel through tension-torsion tests*, Comput. Struct., **83** (2005), 1005–1020.
[39] F. Freddi, G. Royer-Carfagni: *Regularized variational theories of fracture: a unified approach*, J. Mech. Phys. Solids, **58** (2010), 1154–1174.
[40] I. Giorgio: *A variational formulation for one-dimensional linear thermoviscoelasticity*, Math. Mech. Complex Syst., **9** (2022), 397–412.
[41] I. Giorgio, U. Andreaus, D. Scerrato and F. Dell'Isola: *A visco-poroelastic model of functional adaptation in bones reconstructed with bio-resorbable materials*, Biomech. Model. Mechanobiol., **15** (2016), 1325–1343.
[42] I. Giorgio, U. Andreaus, F. Dell'Isola and T. Lekszycki: *Viscous second gradient porous materials for bones reconstructed with bio-resorbable grafts*, Extreme Mech. Lett., **13** (2017), 141–147.
[43] I. Giorgio, M. De Angelo, E. Turco and A. Misra: *A Biot–Cosserat two-dimensional elastic nonlinear model for a micromorphic medium*, Contin. Mech. Thermodyn., **32** (2019), 1357–1369.
[44] I. Giorgio, F. Dell'Isola, U. Andreaus, F. Alzahrani, T. Hayat and T. Lekszytcki: *On mechanically driven biological stimulus for bone remodeling as a diffusive phenomenon*, Biomech. Model. Mechanobiol., **18** (2019), 1639–1663.
[45] I. Giorgio, F. Dell'Isola and A. Misra: *Chirality in 2D Cosserat media related to stretch-micro-rotation coupling with links to granular micromechanics*, Int. J. Solids Struct., **202** (2020), 28–38.
[46] I. Giorgio, R. Grygoruk, F. Dell'Isola and D. Steigmann: *Pattern formation in the three-dimensional deformations of fibered sheets*, Mech. Res. Commun., **69** (2015), 164–171.
[47] I. Giorgio, F. Hild, E. Gerami, F. Dell'Isola and A. Misra: *Experimental verification of 2D Cosserat chirality with stretch-micro-rotation coupling in orthotropic metamaterials with granular motif*, Mech. Res. Commun., **126** (2022), Article ID: 104020.
[48] E. Grande, G. Milani, A. Formisano, B. Ghiassi and F. Fabbrocino: *Bond behaviour of FRP strengthening applied on curved masonry substrates: numerical study*, Int. J. Mason. Res. Innov., **5** (2020), 303–320.
[49] L. Greco, M. Cuomo: *An implicit G1 multi patch B-spline interpolation for Kirchhoff–Love space rod*, Comput. Methods Appl. Mech. Eng., **269** (2014), 173–197.
[50] L. Greco, M. Cuomo: *An isogeometric implicit G1 mixed finite element for Kirchhoff space rods*, Comput. Methods Appl. Mech. Eng., **298** (2016), 325–349.
[51] F. Greco, L. Leonetti, R. Luciano and P. Trovalusci: *Multiscale failure analysis of periodic masonry structures with traditional and fiber-reinforced mortar joints*, Compos. B: Eng., **118** (2017), 75–95.

[52] A. Grimaldi, R. Luciano: *Tensile stiffness and strength of fiber-reinforced concrete*, J. Mech. Phys. Solids, **48** (2000), 1987–2008.
[53] G. Khoury, C. Majorana, F. Pesavento and B. Schrefler: *Modelling of heated concrete*, Mag. Concr. Res.", **54** (2002), 77–101.
[54] D. Kumar, F. Ayant and C. Cesarano: *Analytical Solutions of Temperature Distribution in a Rectangular Parallelepiped*, Axioms, **11** (2022), Article ID: 488.
[55] J. Larsen: *A new variational principle for cohesive fracture and elastoplasticity*, Mech. Res. Commun., **58** (2014), 133-138.
[56] C. Majorana, V. Salomoni and B. Schrefler: *Hygrothermal and mechanical model of concrete at high temperature*, Mater. Struct., **31** (1998), 378–386.
[57] G. Mancusi, F. Fabbrocino, L. Feo and F. Fraternali: *Size effect and dynamic properties of 2D lattice materials*, Compos. B: Eng., **112** (2017), 235–242.
[58] A. Misra, P. Poorsolhjouy: *Granular micromechanics model for damage and plasticity of cementitious materials based upon thermomechanics*, Math. Mech. Solids, **25** (10) (2015), Article ID: 1081286515576821.
[59] A. Misra, V. Singh: *Micromechanical model for viscoelastic materials undergoing damage*, Contin. Mech. Thermodyn., **25** (2013), 343–358.
[60] A. Misra, V. Singh: *Thermomechanics-based nonlinear rate-dependent coupled damage-plasticity granular micromechanics model*, Contin. Mech. Thermodyn., **27** (4-5) (2015), Article ID: 787.
[61] M. M. Nava, R. Fedele and M. T. Raimondi: *Computational prediction of strain-dependent diffusion of transcription factors through the cell nucleus*, Biomech. Model. Mechanobiol., **15** (2016), 983–993.
[62] C. Navier: *Memoire sur les lois de l'equilibre et du mouvement des corps solides elastiques*, Academie des Sciences, (1827).
[63] N. Nejadsadeghi, F. Hild and A. Misra: *Parametric experimentation to evaluate chiral bars representative of granular motif*, Int. J. Mech. Sci., **221** (2022), Article ID: 107184.
[64] N. Nejadsadeghi, A. Misra: *Extended granular micromechanics approach: a micromorphic theory of degree n*, Math. Mech. Solids, **25** (2020), 407–429.
[65] C. Liu, Y. Zhong: *Existence and multiplicity of periodic solutions for nonautonomous second-order discrete Hamiltonian systems*, Constr. Math. Anal., **3** (2020), 178–188.
[66] L. Placidi, E. Barchiesi, A. Misra and D. Timofeev: *Micromechanics-based elasto-plastic–damage energy formulation for strain gradient solids with granular microstructure*, Contin. Mech. Thermodyn., **33** (2021), 2213–2241.
[67] P. Poorsolhjouy, A. Misra: *Effect of intermediate principal stress and loading-path on failure of cementitious materials using granular micromechanics*, Int. J. Solids Struct., **108** (2017), 139–152.
[68] Y. Rahali, I. Giorgio, J. Ganghoffer and F. Dell'Isola: *Homogenization à la Piola produces second gradient continuum models for linear pantographic lattices*, Int. J. Eng. Sci., **97** (2015), 148–172.
[69] G. Ramaglia, G. Lignola, F. Fabbrocino and A. Prota: *Numerical investigation of masonry strengthened with composites*, Polymers, **10** (2018), Article ID: 334.
[70] B. Schrefler, P. Brunello, D. Gawin, C. Majorana and F. Pesavento: *Concrete at high temperature with application to tunnel fire*, Comput. Mech., **29** (2002), 43–51.
[71] D. Scerrato, I. Giorgio, A. Madeo, A. Limam and F. Darve: *A simple non-linear model for internal friction in modified concrete*, Int. J. Eng. Sci., **80** (2014), 136–152.
[72] B. Schrefler, C. Majorana, G. Khoury and D. Gawin: *Thermo-hydro-mechanical modelling of high performance concrete at high temperatures*, Eng. Comput., **19** (2002), 787–819.
[73] P. Seppecher, J. Alibert and F. Dell'Isola: *Linear elastic trusses leading to continua with exotic mechanical interactions*, J. Phys. Conf. Ser., **319** (2011), Article ID: 012018.
[74] J. Simo, T. Hughes: *Computational inelasticity*, Springer Science & Business Media, (2006).
[75] J. Simo, R. Taylor: *Quasi-incompressible finite elasticity in principal stretches. Continuum basis and numerical algorithms*, Comput. Methods Appl. Mech. Eng., **85** (1991), 273–310.
[76] R. Sarikaya, Q. Ye, L. Song, C. Tamerler, P. Spencer and A. Misra: *Probing the mineralized tissue-adhesive interface for tensile nature and bond strength*, J. Mech. Behav. Biomed. Mater., **120** (2021), Article ID:104563.
[77] M. Spagnuolo, K. Barcz, A. Pfaff, F. Dell'Isola and P. Franciosi: *Qualitative pivot damage analysis in aluminum printed pantographic sheets: numerics and experiments*, Mech. Res. Commun., **83** (2017), 47–52.
[78] G. Tocci Monaco, N. Fantuzzi, F. Fabbrocino and R. Luciano: *Semi-analytical static analysis of nonlocal strain gradient laminated composite nanoplates in hygrothermal environment*, J. Braz. Soc. Mech. Sci. Eng., **43** (2021), Article ID: 274.
[79] E. Turco, F. Dell'Isola, N. Rizzi, R. Grygoruk, W. Müller and C. Liebold: *Fiber rupture in sheared planar pantographic sheets: Numerical and experimental evidence*, Mech. Res. Commun., **76** (2016), 86–90.
[80] E. Turco, M. Golaszewski, I. Giorgio and F. D'Annibale: *Pantographic lattices with non-orthogonal fibres: Experiments and their numerical simulations*, Compos. B: Eng., **118** (2017), 1–14.
[81] Y. Yang, A. Misra: *Higher-order stress-strain theory for damage modeling implemented in an element-free Galerkin formulation*, CMES - Comput. Model. Eng. Sci., **64** (1) (2010), 1–36.

[82] Y. Yang, A. Misra: *Micromechanics based second gradient continuum theory for shear band modeling in cohesive granular materials following damage elasticity*, Int. J. Solids Struct., **49** (18) (2012), 2500–2514.

[83] M. E. Yildizdag, L. Placidi and E. Turco: *Modeling and numerical investigation of damage behavior in pantographic layers using a hemivariational formulation adapted for a Hencky-type discrete model*, Contin. Mech. Thermodyn., **35** (2023), 1481–1494.

Luca Placidi
International Telematic University Uninettuno
Section of Mathematics
Corso Vittorio Emanuele II, 39, 00186, Rome, Italy
ORCID: 0000-0002-1461-3997
Email address: luca.placidi@uninettunouniversity.net

Anil Misra
Florida International University
Department of Mathematics and Statistics
Deuxieme Maison, 430, 11101 SW 13th St, Miami, USA
ORCID: 0000-0002-9761-2358
Email address: anmisra@fiu.edu

Abdou Kandalaft
University of Catania
Department of Mathematics and Computer Science
Piazza Università, 2, 95131, Catania, Italy
ORCID: 0000-0002-1556-0540
Email address: abdou.kandalaft@phd.unict.it

Mohammad Mahdi Nayeban
University of Catania
Department of Mathematics and Computer Science
Piazza Università, 2, 95131, Catania, Italy
ORCID: 0009-0000-1302-2901
Email address: mohammad.nayeban@phd.unict.it

Nurettin Yilmaz
Università dell'Aquila
Department of Information Engineering, Computer Science and Mathematics
via Vetoio (Coppito), 1 – 67100 L'Aquila, Italy
ORCID: 0009-0007-9362-0928
Email address: nurettin.yilmaz@graduate.univaq.it